https://doi.org/10.5194/wes-2022-44
Preprint. Discussion started: 27 June 2022

eawe european academy of wind energy
Open Access WIND ENERGY SCIENCE DISCUSSIONS

Brief communication: A momentum-conserving superposition method applied to the super-Gaussian wind turbine wake model

Frédéric Blondel[1]

[1] 1-4 Av. du Bois Préau, 92852 Rueil-Malmaison

Correspondence: Frédéric Blondel (frederic.blondel@ifpen.fr)

Abstract. Accurate wind farm flow predictions based on analytical wake models are crucial for wind farm design and layout optimisation. In this regard, wake superposition methods play a key role and remain a substantial source of uncertainty. Recently, new models based on mass and momentum conservation have been proposed in the literature. In the present work, such methods are extended to the superposition of super-Gaussian type velocity deficit models, allowing the full wake velocity deficit estimation and design of closely packed wind farms.

1 Introduction

Wind farm design and layout optimisation rely on analytical flow models due to a large number of configurations to be evaluated and the computational efficiency of such numerical methods. A typical wind farm flow solver consists of a combination of several sub-models, including *a minima* a velocity deficit model, a wake-added-turbulence (WAT) model, and possibly a wake deflection model, a blockage model, and a coupled wake/atmospheric-boundary-layer model. The velocity deficit and WAT models usually apply to a single wind turbine: wake superposition methods accumulate the wakes and estimate a wind farm power production for given environmental conditions. Concerning the superposition of velocity deficits, the available methods lacked theoretical justification, see Zong and Porté-Agel (2020), until the recent work of Zong and Porté-Agel (2020) and Bastankhah et al. (2021). In these studies, analytical solutions for the velocity deficit superposition are proposed based on the mass and momentum conservation principle. These superposition methods assume Gaussian-shaped velocity deficit profiles. In the present article, the approach of Bastankhah et al. (2021) is extended to super-Gaussian wake velocity deficit profiles. Such models, proposed in Shapiro et al. (2019) and later refined in Blondel and Cathelain (2020), allow for the evaluation of the velocity deficit over the full wake. On the contrary, the Gaussian-based approaches are limited to the far-wake. Apart from preventing the appearance of unrepresentable numbers, this allows the study of closely packed wind farm layouts. Indeed, some offshore wind farms such as Lillgrund exhibit small wind turbine inter-distances, down to 3.3 wind turbine diameters. Considering such super-Gaussian velocity profiles together with the Bastankhah et al. (2021) superposition method, an integral has no analytical solution, and an approximation is proposed and compared with the numerical solution. It is also shown in section 3 that the method proposed in Bay et al. (2022) leads to similar results in terms of centerline velocity deficit and is suited for wind-farm power predictions. The new superposition method has more robust theoretical foundations than

https://doi.org/10.5194/wes-2022-44
Preprint. Discussion started: 27 June 2022

the traditionally used local-linear-sum (LLS) superposition technique (method C in Zong and Porté-Agel (2020)), and its applicability is demonstrated based on the large Horns-Rev wind farm.

2 Extension of the Bastankhah et al. (2021) model

2.1 Model derivation

In Bastankhah et al. (2021), the conservation of momentum deficit for multiple wakes takes the form:

$$\int_{\tilde{A}} \left(u_0 c_n f_n - (c_n f_n)^2 - 2 c_n f_n \sum_{i=1}^{n-1} c_i f_i \right) d\tilde{A} \approx \frac{\tilde{T}_n}{\rho}, \tag{1}$$

with c_n the maximum velocity deficit of turbine n, i the index of the turbine upwind of turbine n, f_n the self-similar function, $\tilde{A} = \pi \tilde{r}^2$ the rotor surface with $\tilde{r} = r/d_0$ and d_0 the wind turbine diameter, $\tilde{T}_n$ the thrust force of the unit diameter rotor, u_0 the undisturbed wind velocity, and ρ the fluid density. Based on comparisons to numerical results from a large-eddy simulation (LES) solver, a modified form was proposed in Bastankhah et al. (2021): the factor two in the left-hand side of Eq. (1) is dropped.

Let us consider the original form, Eq. (1). Given a super-Gaussian shape function f_n, a solution for c_n is sought. Following Blondel and Cathelain (2020), the shape function reads $f_i = \exp\left(-\tilde{r_i}^k / 2\tilde{\sigma_i}^2\right)$, with $k = k(\tilde{x})$ the super-Gaussian order and i or n the index of a wind turbine. In the following, we assume that the turbines are sorted from the most upwind to the most downwind, and for two turbines i and n, we have $i < n$.

Here, the radius $\tilde{r_i} = \sqrt{(y-y_i)^2 + (z-z_i)^2}/d_0$ and the super-Gaussian characteristic width $\tilde{\sigma_i}$ are normalized by the wind turbine diameter d_0, indicated by the tilde. The following integrals are defined in terms of the gamma function Γ:

$$\int_{\tilde{A}} f_n d\tilde{A} = \frac{\pi}{k} \Gamma\left(\frac{2}{k}\right) 2^{2/k+1} \tilde{\sigma}_n^{4/k}, \qquad \textstyle\int_{\tilde{A}} f_n^2 d\tilde{A} = \frac{2\pi}{k} \Gamma\left(\frac{2}{k}\right) \tilde{\sigma}_n^{4/k}, \quad \text{and} \quad \textstyle\int_{\tilde{A}} f_n f_i d\tilde{A} = \mathcal{I}. \tag{2}$$

No analytical solution could be found for the last integral, denoted $\mathcal{I}$. Inserting Eqs. (2) into Eq. (1) leads to:

$$u_0 c_n \frac{\pi}{k} \Gamma\left(\frac{2}{k}\right) 2^{2/k+1} \tilde{\sigma}_n^{4/k} - c_n^2 \frac{2\pi}{k} \Gamma\left(\frac{2}{k}\right) \tilde{\sigma}_n^{4/k} - 2 c_n \sum_{i}^{n-1} c_i \mathcal{I} \approx \frac{\tilde{T}_n}{\rho}. \tag{3}$$

Using the thrust coefficient $C_{T_n} = 8\tilde{T}_n / \left(\pi \rho \tilde{d_0}^2 < U_{n-1} >^2_{(n,x_n)}\right)$, the operator $<>_{(n,x_n)}$ denoting the spatial averaging over the frontal projected area of rotor n at $x = x_n$, as in Bastankhah et al. (2021), one obtains:

$$c_n^2 - c_n 2^{2/k} \left(u_0 - 2 \sum_{i}^{n-1} \frac{c_i}{2^{2/k}} \frac{k\mathcal{I}}{2\pi \Gamma\left(\frac{2}{k}\right) \tilde{\sigma}_n^{4/k}} \right) + \frac{k C_{T_n}}{16} \frac{< u_{n-1} >^2_{(n,x_n)}}{\Gamma\left(\frac{2}{k}\right) \tilde{\sigma}_n^{4/k}} \approx 0. \tag{4}$$

https://doi.org/10.5194/wes-2022-44
Preprint. Discussion started: 27 June 2022

eawe european academy of wind energy
Open Access WIND ENERGY SCIENCE DISCUSSIONS

Let us introduce a modified integral $\mathcal{J} = k\mathcal{I}/\left(2^{2/k}\pi\Gamma\left(\frac{2}{k}\right)\tilde{\sigma}_n^{4/k}\right)$. After straightforward manipulations, and assuming $u_0 = u_h$, i.e., a constant, shear-free inflow, the solution for c_n reads:

$$\frac{c_n}{u_h} = \left(1 - \sum_{i=1}^{n-1}\frac{c_i}{u_h}\mathcal{J}\right)\left(2^{2/k-1} - \sqrt{2^{4/k-2} - \frac{kC_{T_n}\left(\frac{< u_{n-1} >_{(n,x_n)}}{u_h}\right)^2}{16\Gamma\left(\frac{2}{k}\right)\tilde{\sigma}_n^{4/k}\left(1-\sum_{i=1}^{n-1}\frac{c_i}{u_h}\mathcal{J}\right)^2}}\right). \tag{5}$$

The modified form is obtained by using a modified $\mathcal{J}$ together with Eq. (5) and $\mathcal{I}^{mod} = \mathcal{I}/2$:

$$\mathcal{J}^{mod} = \frac{n\mathcal{I}^{mod}}{2^{2/k}\pi\Gamma\left(\frac{2}{k}\right)\tilde{\sigma}_n^{4/k}}. \tag{6}$$

2.2 Approximate solutions of the integral $\mathcal{I}$

In a first approach, one may assume a Gaussian behaviour of the model to evaluate $\mathcal{J}$, as done in Bay et al. (2022). One obtains, see Bastankhah et al. (2021):

$$\mathcal{J}_{Gauss}^{mod} = \frac{\pi\tilde{\sigma}_i^2\tilde{\sigma}_n^2}{\tilde{\sigma}_i^2+\tilde{\sigma}_n^2}\exp\left(-\frac{(\tilde{y}_n-\tilde{y}_i)^2}{2(\tilde{\sigma}_n^2+\tilde{\sigma}_i^2)}\right)\exp\left(-\frac{(\tilde{z}_n-\tilde{z}_i)^2}{2(\tilde{\sigma}_n^2+\tilde{\sigma}_i^2)}\right). \tag{7}$$

Alternatively, one may first consider aligned turbines ($\tilde{y}_i - \tilde{y}_n = 0$, $\tilde{z}_i - \tilde{z}_n = 0$) and later correct the integral for the lateral distance between the rotor using a function $\delta(\tilde{y},\tilde{z})$. This function is identified from the Gaussian solution. A second approximation consists in considering an equivalent super-Gaussian order, $k_{eq} = 1/2\,(k_i + k_n)$. Under these hypotheses, the integral $\mathcal{I}$ takes the form:

$$\mathcal{I}_{kEquiv}^{mod} = \frac{\pi\Gamma\left(2/k_{eq}\right)2^{2/k_{eq}+1}\tilde{\sigma}_i^{4/k_{eq}}\tilde{\sigma}_n^{4/k_{eq}}}{k_{eq}\left(\tilde{\sigma}_i^2+\tilde{\sigma}_n^2\right)^{2/k_{eq}}}\delta(\tilde{y},\tilde{z}), \quad \text{with} \quad \delta(\tilde{y},\tilde{z}) = \exp\left(-\frac{(\tilde{y}_n-\tilde{y}_i)^{k_{eq}}}{2(\tilde{\sigma}_n^2+\tilde{\sigma}_i^2)}\right)\exp\left(-\frac{(\tilde{z}_n-\tilde{z}_i)^{k_{eq}}}{2(\tilde{\sigma}_n^2+\tilde{\sigma}_i^2)}\right), \tag{8}$$

and Eq. (6) is used to calculate $\mathcal{J}_{kEquiv}^{mod}$. Another straightforward approach consists in tabulating the integral values (excluding the $\delta(\tilde{y},\tilde{z})$ function) and linearly interpolating between the data, which is the one retained in practice. For a quantitative comparison, the proposed analytical approximations of the integral $\mathcal{J}$ are compared to the numerical integration. An interval of $0.2 \le \sigma_i, \sigma_n \le 2.5$ is considered for the characteristic width, and several intervals $2 \le k_i, k_n < max_k$ are considered for the super-Gaussian order, with $2 < max_k \le 8$. The bounding values are representative of the very near wake of a wind turbine under laminar flow conditions and the very far wake ($\tilde{x} > 15d_0$) under highly turbulent conditions: the typical operating range of a turbine in a wind farm is covered. Among the characteristic width and super-Gaussian order intervals, 15 values are sampled. Regarding the maximum super-Gaussian order, 6 equally-spaced values are sampled. For each set of four inputs, and for a given maximum super-Gaussian order, the analytical approximations are evaluated, and the error is computed ($error = (|\mathcal{J}_{Analytical}| - |\mathcal{J}_{Numerical}|)\,/\,|\mathcal{J}_{Numerical}|$). The numerical evaluation is based on the scipy (Jones et al. (2001)) "integrate.quad" integration routine, and extends from 0 to $6 \cdot max(\sigma_i, \sigma_n)$. Then, for each max_k, the average and maximal error are computed and reported in Figure 1. From these results, the so-called $kEquiv$ method seemingly outperforms the $Gauss$ method and should be preferred. However, it will be shown in Section 3 that the impact on the velocity deficit is limited.

https://doi.org/10.5194/wes-2022-44
Preprint. Discussion started: 27 June 2022

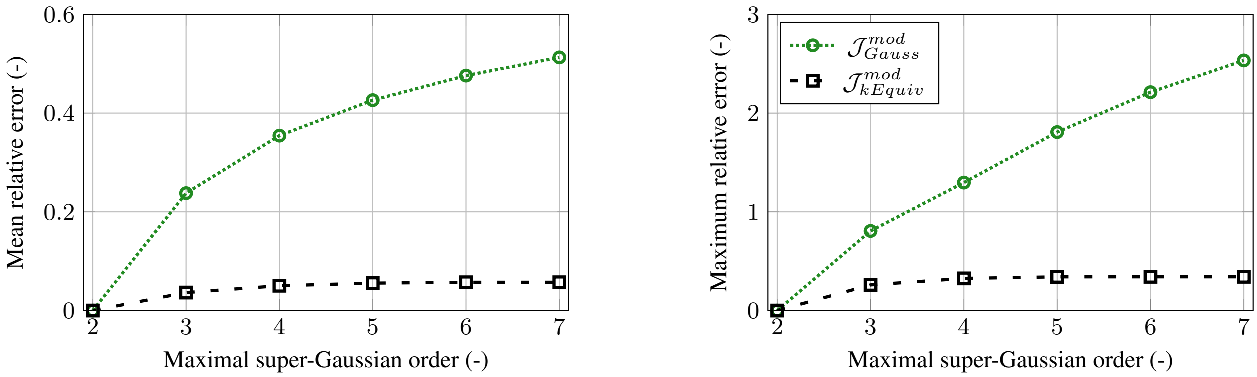

Figure 1. Mean (left) and maximal (right) relative error of the analytical integrals compared with the numerical evaluation of $\mathcal{J}$ as a function of the maximal considered super-Gaussian order

3 Results

Due to the poor performance of the super-Gaussian model noticed in Lanzilao and Meyers (2022), the model has first been re-calibrated, focusing on the far wake, and enforcing $k = 2$ as a boundary condition. The procedure and notations follow the work of Cathelain et al. (2020). Instead of using a root-finding algorithm for a_f, a polynomial approximation is used:

$$a_f = -8.2635C_T^3 + 8.5939C_T^2 - 8.9691C_T + 10.7286 \tag{9}$$

The proposed calibration is not meant to be universal but dedicated to the present study. Future work will be dedicated to a calibration that is reliable in both near and far-wake regions. Table 1 provides the list of the model coefficients used in the present study. As noticed in Figure 2, the increase of the centerline velocity deficit in the very near-wake is not strong

Table 1. Coefficients of the super-Gaussian wake model

a_s	b_s	c_s	a_f	b_f	c_f
0.28	0.01	$0.1 \times C_T + 0.1$	Eq. 9	$1.68\exp(-25.98TI) - 1.06$	2.

enough, inducing a non-smooth transition between the vortex-cylinder-based induction zone and the wake. Furthermore, using the momentum-conserving method, a velocity discontinuity appears at the rotor plane. This is due to the so-called modified formulation. Using the un-modified formulation leads to very high near-wake velocity deficits or even unrepresentable numbers in the presented test case.

https://doi.org/10.5194/wes-2022-44
Preprint. Discussion started: 27 June 2022

eawe european academy of wind energy
Open Access WIND ENERGY SCIENCE DISCUSSIONS

3.1 Comparison against large-eddy simulations from Bastankhah et al. (2021)

For the model comparison, the numerical setup based on the aligned wind farm introduced in Bastankhah et al. (2021) is reproduced. The wind farm flow model builds upon the super-Gaussian model as described in Blondel and Cathelain (2020), using the calibration introduced in section 3. The WAT model proposed in Ishihara and Qian (2018) is employed, together with a so-called “maximum-value" WAT superposition, see Niayifar and Porté-Agel (2016). A correction factor of 1.25 is applied on the maximum of added turbulence to match the results presented in Bastankhah et al. (2021). The rotor disks are discretized based on 12×12 polar grids. The rotor averaged velocity and turbulence intensity are estimated using a local rotor element area ponderated average. A blockage correction based on the vortex cylinder flow model, see Branlard and Meyer Forsting (2020), is used. The LLS method is compared to the present method, denoted MC (Momentum Conserving), with the two approximations for $\mathcal{J}^{mod}$, as well as a direct numerical evaluation of the integral, denoted $\mathcal{J}^{mod}_{Num}$.

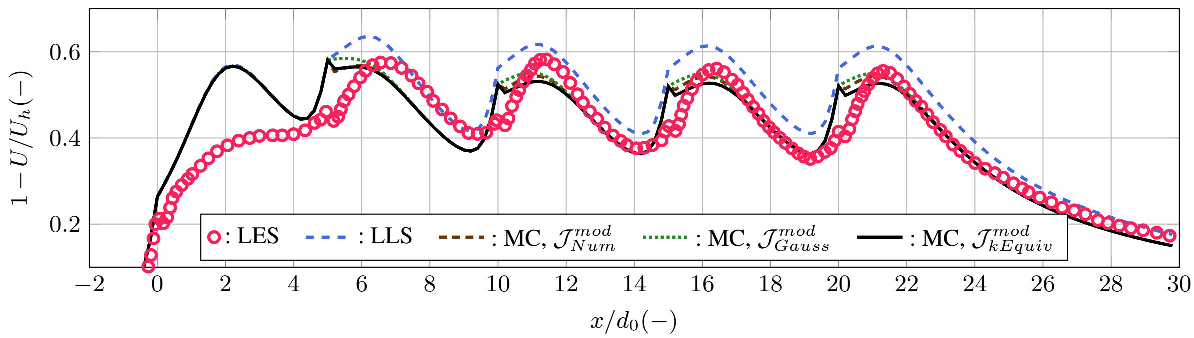

Figure 2. Centerline velocity deficit in the middle column of the farm, LES data scanned from Bastankhah et al. (2021)

Figure 2 shows that, compared with the LLS superposition method, the MC model predicts a lower velocity deficit in both near and far wake regions. Moreover, the proposed analytical approximations of the integral $\mathcal{J}^{mod}$ are very close to the numerical approximation in the presented test case. In the far wake regions, 3 diameters behind the wind turbines, the $\mathcal{J}^{mod}_{kEquiv}$ and $\mathcal{J}^{mod}_{Gauss}$ approximations lead to superimposed velocity deficit, since the super-Gaussian order is close to 2. These observations validate the approach employed in Bay et al. (2022), despite the higher errors noticed in Figure 1. In practice, using a tabulated version of the integral is a fast and convenient approach. However, it does not circumvent the approximation based on the rotor distance function, $\delta(\tilde{y},\tilde{z})$, since tabulating the complete integral results in large data files that are time-consuming to load. The global agreement against the LES dataset is satisfying. In the first turbine wake, the hub effect prevents a proper analysis of the results. For the second turbine, a good agreement is obtained with the LLS method, while the MC method underpredicts the velocity deficit. This behavior, as noted in Bastankhah et al. (2021), is a consequence of the application of the modified momentum conservation law. For the following three turbines, a good agreement is obtained.

https://doi.org/10.5194/wes-2022-44
Preprint. Discussion started: 27 June 2022

WIND ENERGY SCIENCE DISCUSSIONS

3.2 Comparison against large-eddy simulations of the Horns-Rev wind farm from Porté-Agel et al. (2013)

The model predictions are also compared with large-eddy simulations of the Horns-Rev wind farm, as presented in Porté-Agel et al. (2013). With a minimal inter-turbine distance of 7 diameters, this wind farm can not be considered as closely-packed. However, the availability of a large set of large-eddy simulation results makes it a good candidate for validation purposes. Figure 3 compares the wind farm efficiency η (predicted power by theoretical power without wake effect) over a wide range of wind directions θ. We use the LES as a reference to avoid the uncertainties of SCADA measurements, mainly due to the wind direction changes during the $10\,\mathrm{min}$ averaging in the available data. The agreement between the analytical model and the

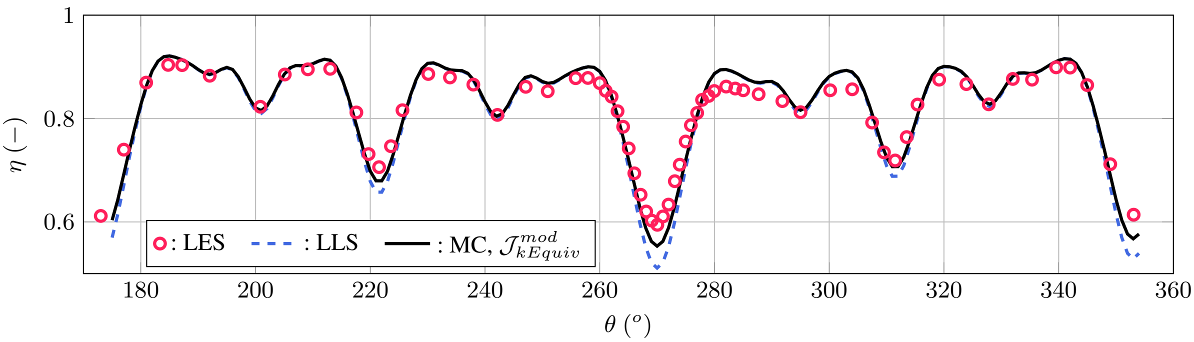

Figure 3. Centerline velocity deficit in the middle column of the farm, LES data scanned from Bastankhah et al. (2021)

LES dataset is overall good. Differences between the momentum-conserving superposition method and the LLS approach are noticed for wind directions where the wake effects are strong, typically at $\theta \approx \{222^o, 270^o, 312^o\}$. Around such directions, the lower velocity deficits predicted by the MC approach lead to lower wake losses and better efficiency of the wind farm.

4 Conclusions

In this work, the momentum-conserving wake superposition method proposed in Bastankhah et al. (2021) was extended to super-Gaussian-type of velocity deficit models. An integral could not be resolved analytically, and an approximation has been proposed. This approximation is closer to numerical evaluations of the integral that the Gaussian assumption used in Bay et al. (2022). Comparisons against large-eddy simulations of wind farms show a satisfactory agreement, allowing the simulation of large wind farms using the super-Gaussian wake model. Further studies will include an extensive validation of the resulting wind farm flow model, including closely-packed wind farms.

Code and data availability. The numerical results based on the analytical models can be made available on demand.

https://doi.org/10.5194/wes-2022-44
Preprint. Discussion started: 27 June 2022

Competing interests. The author declares no competing interests.

Acknowledgements. The author is grateful to Majid Bastankhah for the helpful discussions.

https://doi.org/10.5194/wes-2022-44
Preprint. Discussion started: 27 June 2022

References

Bastankhah, M., Welch, B. L., Martínez-Tossas, L. A., King, J., and Fleming, P.: Analytical solution for the cumulative wake of wind turbines in wind farms, Journal of Fluid Mechanics, 911, A53, https://doi.org/10.1017/jfm.2020.1037, 2021.

Bay, C. J., Fleming, P., Doekemeijer, B., King, J., Churchfield, M., and Mudafort, R.: Addressing deep array effects and impacts to wake steering with the cumulative-curl wake model, Wind Energy Science Discussions, 2022, 1–28, https://doi.org/10.5194/wes-2022-17, 2022.

Blondel, F. and Cathelain, M.: An alternative form of the super-Gaussian wind turbine wake model, Wind Energy Science, 5, 1225–1236, https://doi.org/10.5194/wes-5-1225-2020, 2020.

Branlard, E. and Meyer Forsting, A. R.: Assessing the blockage effect of wind turbines and wind farms using an analytical vortex model, Wind Energy, 23, 2068–2086, https://doi.org/https://doi.org/10.1002/we.2546, 2020.

Cathelain, M., Blondel, F., Joulin, P., and Bozonnet, P.: Calibration of a super-Gaussian wake model with a focus on near-wake characteristics, Journal of Physics: Conference Series, 1618, 062 008, https://doi.org/10.1088/1742-6596/1618/6/062008, 2020.

Ishihara, T. and Qian, G.-W.: A new Gaussian-based analytical wake model for wind turbines considering ambient turbulence intensities and thrust coefficient effects, Journal of Wind Engineering and Industrial Aerodynamics, 177, 275–292, https://doi.org/https://doi.org/10.1016/j.jweia.2018.04.010, 2018.

Jones, E., Oliphant, T., Peterson, P., et al.: SciPy: Open source scientific tools for Python, http://www.scipy.org/, 2001.

Lanzilao, L. and Meyers, J.: A new wake-merging method for wind-farm power prediction in the presence of heterogeneous background velocity fields, Wind Energy, 25, 237–259, https://doi.org/https://doi.org/10.1002/we.2669, 2022.

Niayifar, A. and Porté-Agel, F.: Analytical Modeling of Wind Farms: A New Approach for Power Prediction, Energies, 9, https://doi.org/10.3390/en9090741, 2016.

Porté-Agel, F., Wu, Y.-T., and Chen, C.-H.: A Numerical Study of the Effects of Wind Direction on Turbine Wakes and Power Losses in a Large Wind Farm, Energies, 6, 5297–5313, https://doi.org/10.3390/en6105297, 2013.

Shapiro, C. R., Starke, G. M., Meneveau, C., and Gayme, D. F.: A Wake Modeling Paradigm for Wind Farm Design and Control, Energies, 12, https://doi.org/10.3390/en12152956, 2019.

Zong, H. and Porté-Agel, F.: A momentum-conserving wake superposition method for wind farm power prediction, Journal of Fluid Mechanics, 889, A8, https://doi.org/10.1017/jfm.2020.77, 2020.